Post-buckling Reliability and Sensitivity Analysis of Composite Stiffened Plates Based on Adaptive Kriging Method

Binwen Wang[1] · Lilong Luo[1,2] · Xiaohua Nie[1] · Shihui Duan[1] · Likai Wang[1]

Abstract

Based on the active learning Kriging (ALK) model and the Hashin failure criterion, this paper proposes a new reliability evaluation model for composite stiffened panels, and conducts a reliability analysis on the ultimate bearing capacity. In addition, this paper studies the importance ranking of input variables. By comparing the calculation results of the reliability model proposed in this paper with those of the Monte Carlo method, the accuracy and efficiency of the ALK model are verified by case studies. Finally, the effects of longitudinal elastic modulus and fiber-direction tensile strength on post-buckling failure probability are discussed, which provides significant reference and guidance for the optimization and design of composite stiffened plates.

Keywords Post-bulking reliability analysis · Sensitivity analysis · Composite stiffened plates · Active learning Kriging · Hashin failure criterion

1 Introduction

As a kind of advanced material with special properties, composite materials have been widely used in the aerospace field. By increasing the proportion of composite materials in the main and secondary load-bearing components, the weight reduction effect of aircraft becomes obvious. One of the most common failure forms of thin-walled structures, which are typical components of aircraft structures, is the loss of stability.

As a typical structural form, the stability of plate and shell structures has been studied by many scholars for a long time [1–4]. To analyze the initial failure of composite stiffened plates under axial compression, Orifici et al. [5] adopted the "whole-local" analysis method in the finite element software. Zhou [6] studied the vibration frequency and instability characteristics of ring-stiffened thin-walled cylindrical shells conveying fluid. Additionally, Sun et al. [7] established the topology optimization approach for the stiffener layout of composite stiffened panels based on moving morphable components. These post-buckling analyses of composite stiffened plates are under deterministic conditions, without considering the effect of uncertain parameters.

With the wide application of composite materials, the reliability optimization design of composite materials has been increasingly concerned [8–10]. Due to the nonlinearity of calculating the ultimate bearing capacity of complex composite reinforced panels, the reliability analysis of this structure is time-demanding and inefficient. Traditional post-buckling reliability analysis is based on the first-order reliability method (FORM) or response surface methodology, whose computational budget is expensive and performances are limited by the nonlinearity and cost on finite element analysis of composites. In addition, the in-depth analysis of post-buckling reliability and sensitivity based on the ultimate bearing capacity failure is still lacking. Therefore, in this paper, the reliability model is constructed based on the ultimate bearing capacity failure. Then, the efficient active learning Kriging (ALK) method is first employed to solve the failure probability of composite stiffened plates. And the moment-independent global sensitivity based on the generalized sensitivity idea is first introduced to obtain the importance ranking of input variables, which provides a reference for the design and optimization of composite plates.

The representative approximate analytical methods include the FORM and the second-order reliability method (SORM) [11]. The surrogate model has also evolved greatly [12], such as the Kriging model [13]. The two most famous ALK methods are the efficient global reliability analysis

✉ Lilong Luo
  lilongluo@hotmail.com

1 Aircraft Strength Research Institute of China, Xi'an 710065, China

2 School of Civil Aviation, Northwestern Polytechnical University, Xi'an 710072, China

method proposed by Bichon et al. [14] and the AK-MCS method proposed by Echard et al. Yang et al. [15] combined the ALK model with an IS method based on kernel density estimation to evaluate low failure probability. Gaspar et al. [16] proposed an adaptive Kriging model combining the active refinement and trust region methods. These methods provided a great solving strategy for reliability analysis and low failure probability problems. At the same time, various add-point strategies, also called the active learning functions, were developed, such as the expected feasibility function (EFF) [14], U function[17], expected risk function (ERF) [18], H function[19], and least improvement function (LIF) [20], and so on [21].

Based on failure probability, global sensitivity analysis (GSA) has been employed to measure the influence of uncertainty in random variables on failure probability. The GSA index can be divided into non-parametric index [22], moment-independent index [23] and variance-based index [24]. There are two kinds of moment-independent sensitivity indices. Borgonovo [23] proposed a moment-independent sensitivity index based on differences between the non-conditional and conditional probability density functions (PDF), while Liu and Homma [25] proposed another moment-independent sensitivity index based on differences between the non-conditional and conditional cumulative distribution functions (CDF). To improve the computational efficiency of sensitivity analysis, Guo et al. [26] proposed the variable sensitivity index based on the generalized sensitivity analysis idea. Because the post-buckling reliability problem of composite stiffened plates needs to utilize time-demanding finite element software, this paper derives the efficient moment-independent sensitivity index based on the generalized sensitivity idea.

This paper is organized as follows. Section 2 establishes the post-buckling reliability model and moment-independent global sensitivity index of composite stiffened plates. Section 3 introduces the ALK method for solving post-buckling failure probability and sensitivity index efficiently. Section 4 provides case studies for analyzing the effects of longitudinal elastic modulus and fiber-direction tensile strength on the post-buckling failure probability. Section 5 concludes this paper.

2 Post-buckling Reliability Analysis and Sensitivity Analysis

2.1 Mechanical Properties

The arc-length method is adopted in most finite element software. At present, the improved arc length method [27, 28] has become one of the most important methods for solving nonlinear buckling equations.

For the nonlinear bending problem of composite stiffened plate, the governing equation is as follows

$$[K_T]d\{\Delta\} = d\{P\} \tag{1}$$

where $[K_T], d\{\cdot\}, \Delta$ and P represent tangent stiffness matrix, differential operator, deformation and loaded force, respectively.

$$[K_T] = [K_L] + [K_\sigma] + [K_{NL}] \tag{2}$$

where $[K_L], [K_\sigma]$ and $[K_{NL}]$ indicate linear stiffness matrix, geometric stiffness matrix and initial deformation matrix, respectively.

The Hashin failure criterion is applied to conventional shell elements and continuous shell elements, which can be divided into four failure modes. The detailed expressions are as follows:

Fiber failure mode in tension ($\sigma_{11} > 0$):

$$F_{ft} = \frac{\sigma_{11}^2}{X_T^2} + \alpha\left(\frac{\sigma_{12}}{S_L}\right)^2 = 1 \tag{3}$$

Fiber failure mode in compression ($\sigma_{11} \leq 0$):

$$F_{fc} = \left(\frac{\sigma_{11}}{X_C}\right)^2 = 1 \tag{4}$$

Matrix failure mode in tension ($\sigma_{22} \geq 0$):

$$F_{mt} = \left(\frac{\sigma_{22}}{Y_T}\right)^2 + \left(\frac{\sigma_{12}}{S_L}\right)^2 = 1 \tag{5}$$

Matrix failure mode in compression ($\sigma_{22} \leq 0$):

$$F_{mc} = \left[\left(\frac{Y_C}{2S_T}\right)^2 - 1\right]\frac{\sigma_{22}}{Y_C} + \left(\frac{\sigma_{22}}{2S_T}\right)^2 + \left(\frac{\sigma_{12}}{S_L}\right)^2 = 1 \tag{6}$$

in which, X_T, X_C, Y_T, Y_C, S_L and S_T are axial tensile strength, axial compressive strength, transverse tensile strength, transverse compressive strength, axial shear strength and transverse shear strength, respectively. α is the influential factor of shear strength on fiber failure in tension. σ_{11}, σ_{22} and σ_{12} are the components of effective stress σ.

When the coefficient of damage criterion reaches 1, damage appears in the rubber layer, and its expression is:

$$\left(\frac{\langle\sigma_n\rangle}{N_{\max}}\right)^2 + \left(\frac{\sigma_s}{S_{\max}}\right)^2 + \left(\frac{\sigma_t}{T_{\max}}\right)^2 = 1 \tag{7}$$

where σ_n, σ_s and σ_t are the normal stress, the shear stress in the first direction and the shear stress in the second direction at the opening, respectively. $N_{\max}, S_{\max}$ and $T_{\max}$ represent

the values of normal tensile strength and shear strength in different directions, respectively. The BK failure criterion is utilized to simulate the failure of the adhesive layer after damage. The expression of BK failure criterion is:

$$G_{IC} + (G_{\Pi C} - G_{IC})\left(\frac{G_\Pi}{G_T}\right)^\eta = G_{TC} \tag{8}$$

where G_I, G_Π and G_T are the energy release rates of type I, type Π and the entire model, respectively, and $G_T = G_I + G_\Pi$. G_{IC}, $G_{\Pi C}$ and G_{TC} are the critical energy release rates of type I, type Π and the entire model, respectively, and $G_{TC} = G_{IC} + G_{\Pi C}$.

2.2 Post-buckling Reliability Model

It is assumed that the composite stiffened plate completely fails when its ultimate bearing capacity is reached, so the performance function under axial compression is defined as

$$G(X) = \eta_u P_u(X) - P \tag{9}$$

where $G(X)$ is the performance function, X is the random variable vector included in the reliability evaluation, η_u is the model uncertainty coefficient, P_u is the ultimate bearing capacity, and P is the loaded compression. Eq. (9) contains the ultimate bearing capacity P_u, which is obtained using the nonlinear finite element method (FEM).

In order to improve the calculation efficiency, the ratio coefficient K is introduced and the ultimate strength P_u can be calculated in combination with the buckling load, i.e.

$$P_u = K P_{cr} \tag{10}$$

According to Eq. (10), a new performance function replacing the ultimate compressive strength with buckling load is established for post-buckling reliability analysis, which is defined as

$$G(X) = \eta_u K(X) P_{cr}(X) - P \tag{11}$$

where P_{cr} indicates the buckling load function, and the ratio coefficient $K(X)$ can be defined as

$$K(X) = K_0 h_0(X) \tag{12}$$

where $h_0(X)$ is the distribution function of ratio coefficient K, and K_0 is the mean value of coefficient K, which is obtained by the following equation

$$K_0 = \frac{\overline{P_u}}{\overline{P_{cr}}} \tag{13}$$

where $\overline{P_u}$ is the mean value of the ultimate compression, and $\overline{P}_{cr}$ is the mean buckling load. The distribution function $h_0(X)$ is a function of variables X_T, X_C, Y_T, Y_C, S, R, X_{TC}, S_C.

2.3 Moment-Independent Global Sensitivity Analysis

In order to measure the influence of input variable X_i on the uncertainty of output response, the moment-independent sensitivity index is defined as follows [23, 29–31]

$$\delta_i = \frac{1}{2} E_{X_i}(s(X_i)) = \frac{1}{2} \int s(x_i) f_{X_i}(x_i) \mathrm{d}x_i \tag{14}$$

where $E_{X_i}(\cdot)$ is the expectation operator, $f_{X_i}(x_i)$ indicates the PDF of variable X_i, and $s(X_i)$ is the area difference between the unconditional PDF $f_Y(y)$ and the conditional PDF $f_{Y|X_i}(y)$ of Y, which is as follows

$$s(X_i) = \int \left| f_Y(y) - f_{Y|X_i}(y) \right| \mathrm{d}y \tag{15}$$

where $f_{Y|X_i}(y)$ represents the PDF of the model output Y when the input variable X_i is fixed at x_i, while $f_Y(y)$ is the unconditional PDF of Y. If X_i has greater influence on the uncertainty of Y, fixing X_i will make the PDF of the model output change more, and then the corresponding distance between $f_{Y|X_i}(y)$ and $f_Y(y)$ will be larger, resulting in a larger $s(X_i)$. $s(X_i)$ is a unary function of X_i, and the average influence of X_i on Y can be measured by taking expectation of $s(X_i)$, thus the sensitivity index δ_i can be obtained.

3 Active Learning Kriging Method

As an unbiased estimation model with minimum variance, the Kriging surrogate model combines the global approximation with the local random error.

The Kriging model includes the linear regression model and the stochastic process model, i.e.

$$g(x) = F(x, \beta) + z(x) = \beta + z(x) \tag{16}$$

where $g(x)$ represents the unknown function to fit, β represents the global estimation of the model, and $z(x)$ denotes the random distribution of the unknown function.

Given the design of experiments (DoE), the predicted value and variance of the Kriging model at the unknown point can be expressed as:

$$\mu_g(x) = \hat{\beta} + r(\theta, x)^\mathrm{T} R(\theta)^{-1}\left(g - \hat{\beta}\mathbf{1}\right) \tag{17}$$

$$\sigma_g^2(\boldsymbol{x}) = \sigma^2 \left[1 + \frac{\left(\boldsymbol{1}^{\mathrm{T}} \boldsymbol{R}(\theta)^{-1} \boldsymbol{r}(\theta, \boldsymbol{x}) - 1 \right)^2}{\boldsymbol{1}^{\mathrm{T}} \boldsymbol{R}(\theta)^{-1} \boldsymbol{1}} - \boldsymbol{r}(\theta, \boldsymbol{x})^{\mathrm{T}} \boldsymbol{R}(\theta)^{-1} \boldsymbol{r}(\theta, \boldsymbol{x}) \right]$$

(18)

where $\boldsymbol{1}$ is an m-dimensional unit column vector; $\boldsymbol{r}(\theta, \boldsymbol{x})$ represents the correlation function of training points; $\boldsymbol{R}(\theta)$ is a correlation matrix of any pair of training points; $\hat{\beta}$, σ^2 and θ are parameters of the Kriging model.

With an optimization problem, the estimated value θ solved for can establish a Kriging model:

$$\theta^* = \arg \min_{\theta} \left(|\boldsymbol{R}(\theta)|^{\frac{1}{m}} \sigma^2 \right)$$

(19)

The Kriging interpolation model is established by random sampling of the points near the predicted ones, so the accuracy of the model is bound to be related to the selected sample points. Since the predicted value $\mu_G(x)$ given by the Kriging model is not the real value, there exists a situation where the symbol of the predicted value is different from the real one. The following is a case for separate consideration. When $\hat{G}(x) < 0$, i.e., $\mu_G(x) < 0$, then there is a risk with the real value $G(x) > 0$, and the risk index $\Re(x)$ is defined as

$$\Re(x) = \max[(G(x) - 0), 0]$$

(20)

$\Re(x)$ represents the degree of the true value $G(x) > 0$ when $\mu_G(x) < 0$. Since $G(x)$ is a random variable, $\Re(x)$ is also a random variable. Therefore, the mathematical expectation of $\Re(x)$ is

$$\begin{aligned} E(\Re(x)) &= E[\max((G(x) - 0), 0)] \\ &= \int_0^{+\infty} G(x) \phi\left(\frac{\hat{G}(x) - \mu_G(x)}{\sigma_G(x)} \right) \mathrm{d}G \\ &= \sigma_G(x) \phi\left(\frac{\mu_G(x)}{\sigma_G(x)} \right) + \mu_G(x) \Phi\left(\frac{\mu_G(x)}{\sigma_G(x)} \right) \end{aligned}$$

(21)

where $\mu_G(x)$ is the mean value of the predicted value at point x, and $\sigma_G(x)$ is the variance of the predicted value. $\phi(\cdot)$ is the PDF of the standard normal distribution, and $\Phi(\cdot)$ is the CDF of the standard normal distribution. Similarly, when $\hat{G}(x) > 0$, $\mu_G(x) > 0$, then there is a risk with the true value $G(x) < 0$.

The expected risk equations in separate conditions can be rewritten in a unified form as follows

$$\begin{aligned} E(\Re(x)) &= -\mathrm{sign}(\mu_G(x)) \mu_G(x) \Phi\left(-\mathrm{sign}(\mu_G(x)) \frac{\mu_G(x)}{\sigma_G(x)} \right) \\ &\quad + \sigma_G(x) \phi\left(\frac{\mu_G(x)}{\sigma_G(x)} \right) \end{aligned}$$

(22)

Equation (22) is called the expected risk function (ERF), also known as the learning equation, which illustrates the possibility that the sign of the function to be fitted is predicted wrongly. The basic steps for calculating the post-buckling failure probability and the variable importance ranking of composite stiffened plates by the ALK method are as follows:

Step 1: According to the variable information, generate 20 sample points $X_t = (X_{1,t}, X_{2,t}, \cdots, X_{n,t})(t = 1, 2, \cdots, N, N = 20)$ randomly by the Latin hypercube sampling method and construct the initial set of samples. Then calculate the corresponding values of performance function $G(X)$ with the initial samples. The initial training points and the corresponding responses of $G(X)$ constitute the initial DoE.

Step 2: Generate 10^5 samples randomly in the uncertainty space of input variables as the candidate population.

Step 3: Construct the initial Kriging model with the initial DoE.

Step 4: Predict the values of $\mu_G(X)$ and variances $\sigma_G^2(x)$ of the candidate points using the Kriging model, and then calculate the ERF values based on Eq. (22). The point with the maximum ERF value is marked as X^*.

Step 5: If the maximum value of ERF meets the threshold of convergence condition, then turn to Step 6. The threshold is set as 10^{-3}. Elsewise, add the marked point X^* and its response of performance function into the set of training samples. Refresh the Kriging model with the updated DoE and return to Step 4.

Step 6: Based on the established Kriging model, calculate the post-buckling failure probability by the MCS method.

Step 7: Select failure sample $\left\{ \boldsymbol{x}_1^F, \boldsymbol{x}_2^F, \cdots, \boldsymbol{x}_{N_F}^F \right\}$ to estimate the conditional probability density $f_{x_j}(x_j | F)$ of input variable $\boldsymbol{x}_j$, and label it as $\widehat{f}_{x_j}(x_j | F)$, where N_F is the number of failure samples.

Step 8: According to Eq. (14), estimate δ_i.

4 Case Study

The geometric schematic is shown in Fig. 1. The information of each layer is shown in Table 1, and the thickness of a single layer is 0.12 mm.

The material of this composite stiffened plate is CCF300/BA9916, and the material of interface adhesive layer is J116B. Table 2 shows the material properties of J116B and CCF300/BA9916.

In order to verify the accuracy of the finite element model, the simulation results are compared with the experimental ones in reference [32]. A total of 5 sets of tests were carried out, and 5 sets of failure loads were obtained, the mean value of which was 1188.4 kN [32].
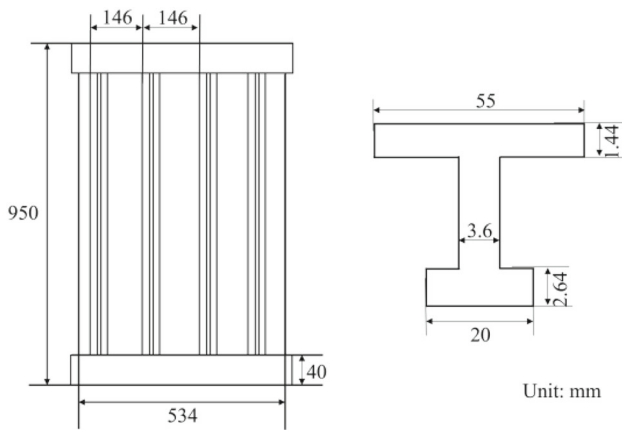
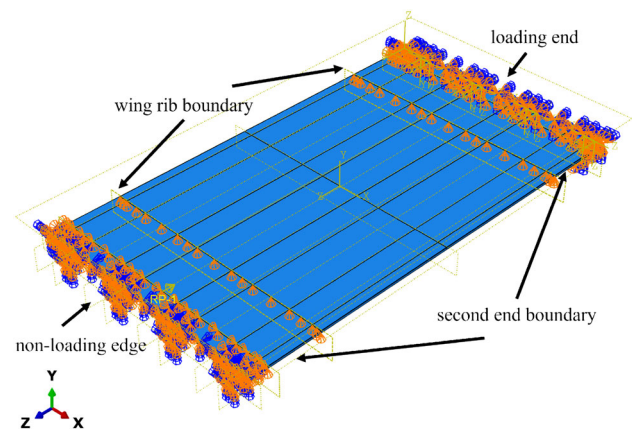Fig. 1 Geometric schematic of the composite stiffened plate

Fig. 2 Finite element model and boundary conditions of stiffened composite plate

In the finite element model, the stiffener and skin are simulated by the shell element (S4R), the adhesive layer is simulated by the cohesive force element, and the cohesive force element and shell element are connected at common nodes. In order to accurately simulate the failure process of composite materials, the Hashin failure criterion is adopted and the damage evolution law is set. The finite element model and boundary conditions of the composite stiffened plate are shown in Fig. 2. As shown in Fig. 2, it is fixed away from the loading end, and the secondary end boundary is constrained by U1 and U2. The wing rib boundary is constrained by the Y-degree of freedom of the plate, and the non-loading edge is free. In the nonlinear analysis of post-buckling, the ninefold first-order bucking modes and onefold second-order buckling modes are used to replace the initial defects.

Figure 3 is the displacement cloud of post-buckling finite element analysis. It can be seen from the figure that the failure area and sequence of finite element analysis are consistent with the experimental results [32].

Figure 4 shows the load–displacement curve of post-buckling analysis, which is obtained by constructing coupling reference points. The final bearing capacity of the structure, i.e., the ultimate load, is 1177.38 kN. And the error of the simulation result compared with the experimental result is 0.93%.

In this paper, all material property parameters of the composite stiffened plate are taken as random variables. Table 3 shows the probabilistic characteristics of each variable. The ultimate strength P is set as 1188.4 kN.

Table 1 Layer information of the composite stiffened plate

Component	Layer information
Skin	$[45/0/-45/90/\pm45/0_2/45_2/0/-45_2/0/45_2/90/-45_2/0]_s$
Horizontal edge strip width (1.44)	$[45/0_3/-45/90]_s$
Horizontal edge strip width (2.64)	$[45/0_2/-45/0_2/-45/0_2/-45/90]_s$
Edge strip heigh (3.6)	$[45/0_2/45/0_2/-45/90/-45/0_2/-45/0_2/45]_s$

Table 2 Mechanical properties of J116B and CCF300/BA9916

Material	Elastic modulus	Strength parameters	Fracture toughness
J116B	$E = 2000$ MPa	$\sigma_{u,\mathrm{I}} = 10$ MPa	$G_{\mathrm{IC}} = 0.252$ N·mm
	$v = 0.382$	$\sigma_{u,\mathrm{II}} = 24.5$ MPa	$G_{\mathrm{IIC}} = 0.665$ N·mm
		$\sigma_{u,\mathrm{III}} = 24.5$ MPa	$G_{\mathrm{IIIC}} = 0.665$ N·mm
CCF300/BA9916	$E_1 = 129$ GPa	$X_T = 1720$ MPa	
	$E_2 = 9.82$ GPa	$X_C = 1230$ MPa	
	$G_{12} = G_{13} = 5.29$ GPa	$Y_T = 70$ MPa	
	$G_{23} = 3.43$ GPa	$Y_C = 220$ MPa	
	$v_{12} = 0.311$	$S_{12} = S_{23} = 134$ MPa	

Fig. 3 Displacement cloud of post-buckling finite element analysis
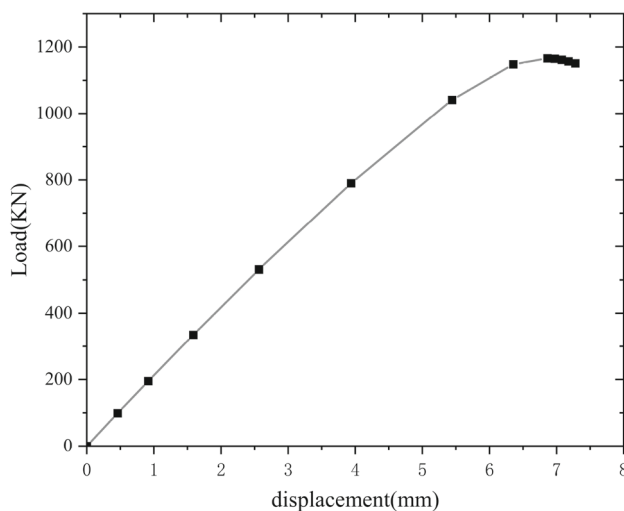
Table 3 Probabilistic properties of fundamental variables

Variable	Type	Mean	Standard deviation
E_1(GPa)	Normal	129	6.45
E_2(GPa)	Normal	9.82	0.491
v_{12}	Normal	0.311	0.016
G_{12}(MPa)	Normal	5290	264.5
G_{13}(MPa)	Normal	5290	264.5
G_{23}(MPa)	Normal	3430	171.5
X_T(MPa)	Normal	1720	86
X_C(MPa)	Normal	1230	61.5
Y_T(MPa)	Normal	70	3.5
Y_C(MPa)	Normal	220	11
S_{23}(MPa)	Normal	134	6.7
S_{12}(MPa)	Normal	134	6.7
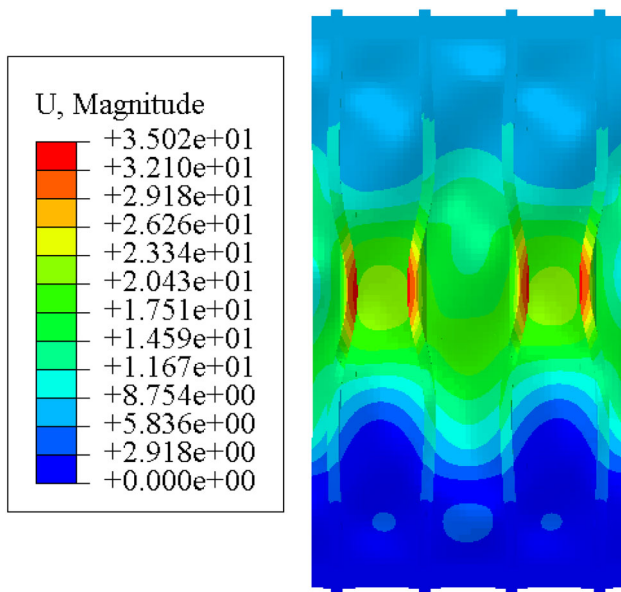
Fig. 4 Load–displacement curve of post-buckling analysis

4.1 Effect of Longitudinal Elastic Modulus

Consider four cases of E_1: (1)$E_1 = 129$ GPa, (2)$E_1 = 140$ GPa, (3)$E_1 = 150$ GPa, and (4)$E_1 = 170$ GPa. And the fiber-direction tensile strength X_T is set as 1720 MPa. The post-buckling failure probability results of these four cases are shown in Table 4. It can be seen that the post-buckling failure probability of composite stiffened plates decreases rapidly with the increase of E_1. When E_1 grows to 170 GPa, the failure probability is only 0.0800, which shows that the fiber is a significant load-bearing part in the structure. The ALK method calls the performance function 154 times in total. The comparison between the results of the ALK method

and the MCS method fully demonstrates the accuracy and efficiency of the ALK method in dealing with post-buckling reliability problems.

For purposes of convenience, the importance rankings of input variables obtained by sensitivity analysis with the increase of longitudinal elastic modulus E_1 are shown in Fig. 5. It can be seen that the sensitivity indices of G_{12}, G_{13} and G_{23} are the largest, and $G_{12} > G_{23} > G_{13}$, which validates that the ability to resist shear failure is significant for composite stiffened plates. In addition, as can be seen from Fig. 5, the importance ranking of E_1 increases with the increase of E_1. When $E_1 = 129$ GPa, $E_1 < v_{12}$; but when $E_1 = 150$ GPa, $E_1 > v_{12}$. This indicates that the contribution of design variables to the post-buckling failure probability of composite stiffened plates varies under various working conditions. However, the importance rankings of $X_T, X_C, Y_T, Y_C, S_{23}$ and S_{12} are smaller and close to zero under various working conditions. In order to verify the rationality of the sensitivity analysis results, the change of failure probability varying with X_T is studied in Sect. 4.2.

4.2 Effect of Fiber-Direction Tensile Strength

Consider four cases of X_T: (1)$X_T = 1720$ MPa, (2)$X_T = 1750$ MPa, (3)$X_T = 1900$ MPa, and (4)$X_T = 2100$ MPa. And the longitudinal elastic modulus E_1 is set as 129 GPa. The results of post-buckling failure probability of these four cases are shown in Table 5. It can be seen that the failure probability of the composite stiffened plate does not change with the increase of X_T, which illustrates that the uncertainty of variable X_T has little effect on the failure probability and further demonstrates the rationality and effectiveness of the sensitivity analysis results in Fig. 5. Therefore, researchers do not need to spend a lot of sources on the tensile strength

Table 4 Post-buckling failure probability of composite stiffened plate with different E_1

Case	E_1(GPa)	ALK		MCS	
		P_f	Function calls	P_f	Function calls
1	129	0.2048	20 + 65	0.2010	10^5
2	140	0.1351	20 + 69	0.1362	
3	150	0.0800	20 + 83	0.0827	
4	170	0.0117	20 + 134	0.0105	

(a) E_1=129 GPa

(b) E_1=140 GPa

(c) E_1=150 GPa

(d) E_1=170 GPa
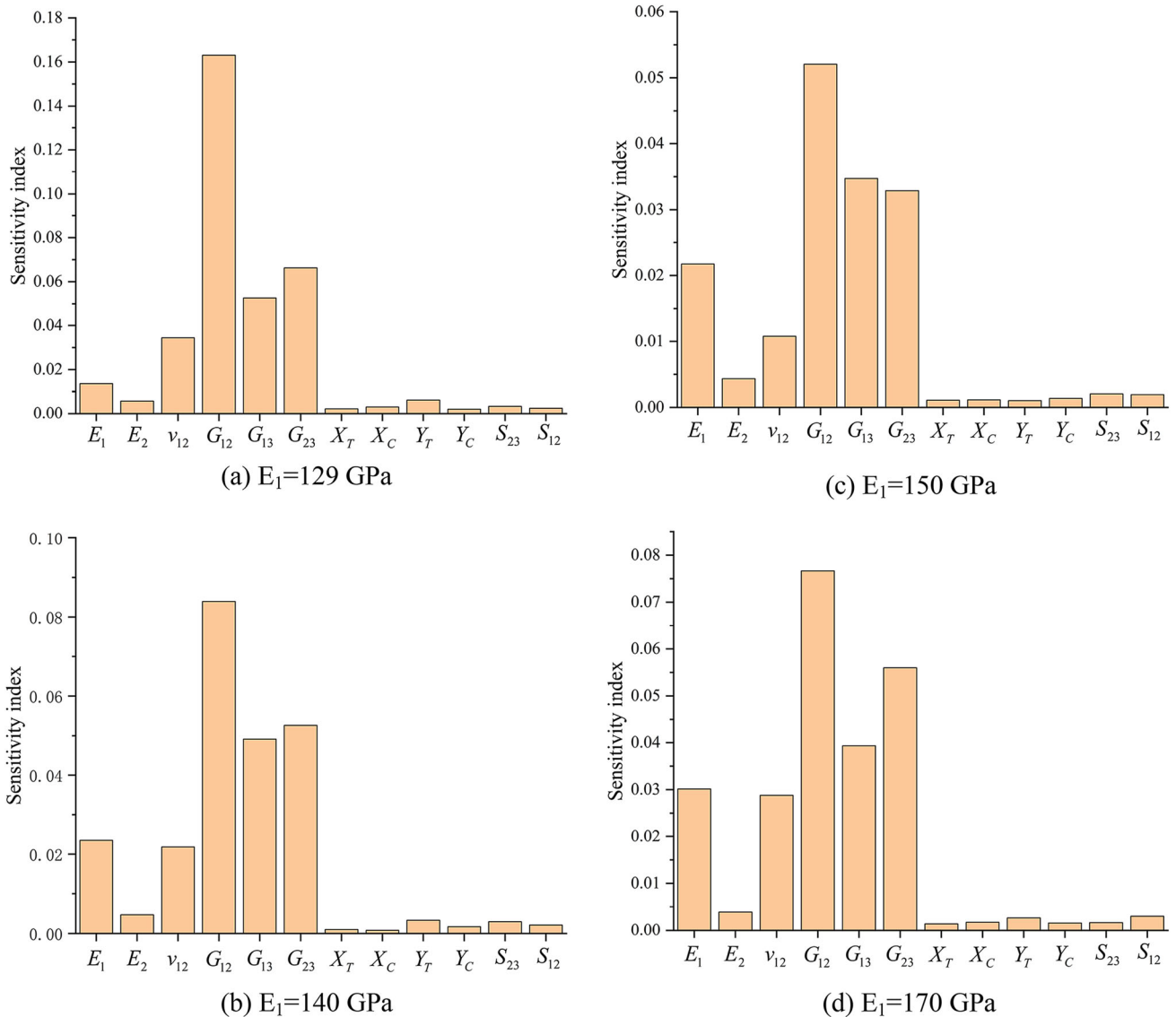
Fig. 5 Sensitivity results of input variables

in the process of reliability design for the ultimate strength of composite stiffened plates. Due to little change of post-buckling failure probability with varying X_T, the sensitivity analysis results with different cases of X_T are not shown in this paper.

5 Conclusion

In this paper, a post-buckling reliability analysis method of composite stiffened plates is proposed based on the ALK model and the Hashin failure criterion. The ALK method is employed to estimate the post-buckling failure probability

Table 5 Post-buckling failure probability of composite stiffened plate with different X_T

Case	X_T (MPa)	ALK		MCS	
		P_f	Function calls	P_f	Function calls
1	1720	0.2048	20 + 62	0.2010	1×10^5
2	1750	0.2105	20 + 60	0.2013	
3	1900	0.2016	20 + 63	0.2011	
4	2100	0.1997	20 + 65	0.2008	

and sensitivity index of composite stiffened plates. In case studies, the simulation accuracy of the finite element model is first verified by comparing the simulation results with the experimental results. The MCS method is employed to obtain the benchmark results for validating the computational accuracy and efficiency of the ALK method. The results show that the ALK method can reduce the computational cost obviously while ensuring the computational accuracy. Then, the effects of longitudinal elastic modulus E_1 and fiber-direction tensile strength X_T on the post-buckling failure probability are analyzed. The sensitivity results show that the shear modulus has the largest effect on the post-buckling reliability of the composite stiffened plate. The variables, whose sensitivity indices are close to zero, can be ignored in the design and optimization of composite stiffened plates, which is further demonstrated in the investigation of the effect of fiber-direction tensile strength on the post-buckling reliability. The proposed post-buckling reliability and sensitivity analysis method with the ALK model is significant for the safety assessment and optimization design of composite stiffened plates.

Data Availability The raw/processed data required to reproduce these findings cannot be shared at this time as the data also forms part of an ongoing research project.

Declarations

References

1. Chang FK, Chang KY. A progressive damage model for laminated composites containing stress-concentrations. J Compos Mater. 1987;21:834–55.
2. Chang FK, Scott RA, Springer GS. Failure strength of nonlinearly elastic composite laminates containing a pin loaded hole. J Compos Mater. 1984;18:464–77.
3. Stevens KA, Ricci R, Davies GAO. Buckling and postbuckling of composite structures. Composites. 1995;26:189–99.
4. Kong CW, Lee IC, Kim CG, Hong CS. Postbuckling and failure of stiffened composite panels under axial compression. Compos Struct. 1998;42:13–21.
5. Orifici AC, Shah SA, Herszberg I, Kotler A, Weller T. Failure analysis in postbuckled composite T-sections. Compos Struct. 2008;86:146–53.
6. Zhou X. Vibration and stability of ring-stiffened thin-walled cylindrical shells conveying fluid. Acta Mech Solida Sin. 2012;25:168–76.
7. Sun Z, Cui R, Cui T, Liu C, Shi S, Guo X. An optimization approach for stiffener layout of composite stiffened panels based on moving morphable components (MMCs). Acta Mech Solida Sin. 2020;33:650–62.
8. Chiachio M, Chiachio J, Rus G. Reliability in composites - a selective review and survey of current development. Compos Part B-Eng. 2012;43:902–13.
9. Blake JIR, Shenoi RA, Das PK, Yang N. The application of reliability methods in the design of stiffened FRP composite panels for marine vessels. Ships Offshore Struct. 2009;4:287–97.
10. Akula VMK. Multiscale reliability analysis of a composite stiffened panel. Compos Struct. 2014;116:432–40.
11. Low BK. FORM, SORM, and spatial modeling in geotechnical engineering. Struct Saf. 2014;49:56–64.
12. Gan N, Li G, Gu J. Hybrid meta-model based design space differentiation method for expensive problems. Acta Mech Solida Sin. 2016;29:120–32.
13. Gaspar B, Teixeira AP, Soares CG. Assessment of the efficiency of Kriging surrogate models for structural reliability analysis. Probab Eng Mech. 2014;37:24–34.
14. Bichon BJ, Eldred MS, Swiler LP, Mahadevan S, McFarland JM. Efficient global reliability analysis for nonlinear implicit performance functions. Aiaa J. 2008;46:2459–68.
15. Yang X, Liu Y, Mi C, Wang X. Active learning Kriging model combining with kernel-density-estimation-based importance sampling method for the estimation of low failure probability. Journal of Mechanical Design. 2018;140.
16. Gaspar B, Teixeira AP, Guedes SC. Adaptive surrogate model with active refinement combining Kriging and a trust region method. Reliab Eng Syst Saf. 2017;165:277–91.
17. Echard B, Gayton N, Lemaire M. AK-MCS an active learning reliability method combining Kriging and Monte Carlo Simulation. Struct Saf. 2011;33:145–54.

18. Yang X, Liu Y, Gao Y, Zhang Y, Gao Z. An active learning kriging model for hybrid reliability analysis with both random and interval variables. Struct Multidiscip Optim. 2014;51:1003–16.

19. Lv Z, Lu Z, Wang P. A new learning function for Kriging and its applications to solve reliability problems in engineering. Comput Math Appl. 2015;70:1182–97.

20. Sun Z, Wang J, Li R, Tong C. LIF: a new Kriging based learning function and its application to structural reliability analysis. Reliab Eng Syst Saf. 2017;157:152–65.

21. Lelièvre N, Beaurepaire P, Mattrand C, Gayton N. AK-MCSi: a Kriging-based method to deal with small failure probabilities and time-consuming models. Struct Saf. 2018;73:1–11.

22. Helton JC, Johnson JD, Sallaberry CJ, Storlie CB. Survey of sampling-based methods for uncertainty and sensitivity analysis. Reliab Eng Syst Saf. 2006;91:1175–209.

23. Borgonovo E. A new uncertainty importance measure. Reliab Eng Syst Saf. 2007;92:771–84.

24. Sobol IM. Theorems and examples on high dimensional model representation. *Reliability Engineering & System Safety* 2003; 79: 187–193 (Pii s0951–8320(02)00229–6).

25. Liu Q, Homma T. A new computational method of a moment-independent uncertainty importance measure. Reliab Eng Syst Saf. 2009;94:1205–11.

26. Guo Q, Liu YS, Chen BQ, Yao Q. A variable and mode sensitivity analysis method for structural system using a novel active learning Kriging model. *Reliability Engineering & System Safety* 2021; 206 (107285).

27. Lam WF, Morley CT. Arc-length method for passing limit points in structural calculation. J Struct Eng-Asce. 1992;118:169–85.

28. Crisfield MA. An arc-length method including line searches and accelerations. Int J Numer Meth Eng. 1983;19:1269–89.

29. Borgonovo E, Castaings W, Tarantola S. Moment independent importance measures: new results and analytical test cases. Risk Anal. 2011;31:404–28.

30. Guo Q, Liu Y, Zhao Y, Li B, Yao Q. Improved resonance reliability and global sensitivity analysis of multi-span pipes conveying fluid based on active learning Kriging model. Int J Press Vessels Pip. 2019;170:92–101.

31. Zhang Y, Liu Y, Yang X, Yue Z. A global nonprobabilistic reliability sensitivity analysis in the mixed aleatory–epistemic uncertain structures. Proc Inst Mech Eng Part G J Aerosp Eng. 2014;228:1802–14.

32. Wang B, Ai S, Zhang G, Nie X, Wu C. Validation method for post-buckling analysis model of stiffened composite panel considering uncertainties. Acta Aeronautica et Astronautica Sinica. 2020;41: 223987.